Transactions of The Indian Institute of Metals
Vol. 62, Issue 2, April 2009, pp. 95-103

Detonation sprayed WC-Co coatings: unique aspects of their structure and mechanical behaviour

G. Sundararajan and P. Suresh Babu

International Advanced Research Centre for Powder Metallurgy & New Materials, Hyderabad-500005 India

Email: director@arci.res.in

Received 11 April 2008
Revised 26 December 2008
Accepted 2 January 2009
Online at www.springerlink.com

Keywords:
thermal spray coatings; detonation spray coatings; WC-Co; decarburization; bond strength

Abstract

Tungsten Carbide-Cobalt (WC-Co) Cermets are known for their excellent wear resistance. Conventionally, WC-Co cermets are produced by liquid phase sintering and such a process results in optimum combination and distribution of WC and Co phases and thus a good combination of hardness and toughness. In contrast to using bulk WC-Co, there are many applications wherein a thick coating of WC-Co over the surface of the engineering component (usually made from steel) represents a cost-effective option. Numerous thermal spray coating techniques have been extensively used to deposit thick WC-Co coatings on a variety of components and detonation spray coating represents one such coating technique capable of depositing hard and dense WC-Co coatings. However, as compared to bulk WC-Co, detonation sprayed WC-Co exhibit inferior properties and performance primarily because of the nature of the detonation spray coating process. In addition, depositing a WC-Co coating on a component automatically introduces an interface between the coating and the substrate and the properties of this interface also become important in determining the overall performance of the WC-Co coating. The purpose of this article is to describe in detail the unique aspects of the structure and mechanical behaviour of detonation sprayed WC-Co coatings and contrast the same with the behaviour of bulk, liquid-phase sintered WC-Co cermet.

1. Introduction

Hard metals, also known as cemented carbides or cermets, represent a group of materials consisting of mixtures of one or more carbides of tungsten, titanium, tantalum and vanadium embedded in a matrix (or binder) of cobalt or nickel. The carbides usually in the form of cuboids account for anywhere from 60 to 95 volume percent of the material volume with the binder phase occupying the remaining volume as illustrated in Fig. 1. Cemented carbides are usually obtained in bulk form through the liquid phase sintering route and have found extensive applications as cutting tools, wear resistant liners and inserts, mining tools and metal forming tools. Among the cemented carbides, the most widely used is the one based on WC as the carbide and Co as the binder phase. The Co content in WC-Co cemented carbide ranges from 6 to 40 volume percent with the balance 94 to 60% constituting the carbide phase. The properties of the WC-Co cemented carbide depends primarily on the Co phase content, WC cuboid size, inter-cuboid spacing and also on the contiguity between the WC phases. It has been observed that the toughness (indentation toughness) of WC-Co can

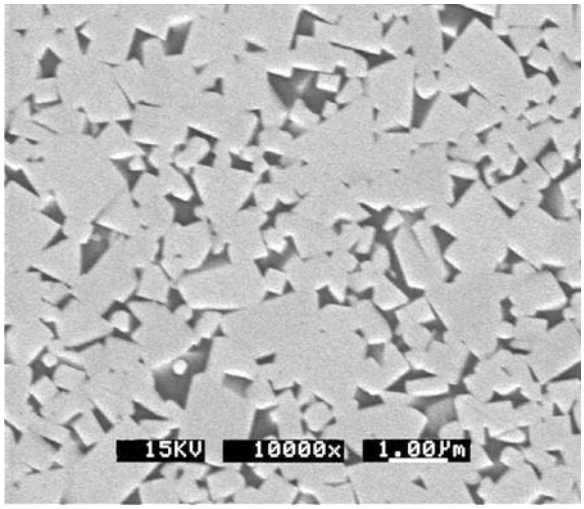

Fig. 1 : SEM image of liquid phase sintered WC-10%Co Cermet.

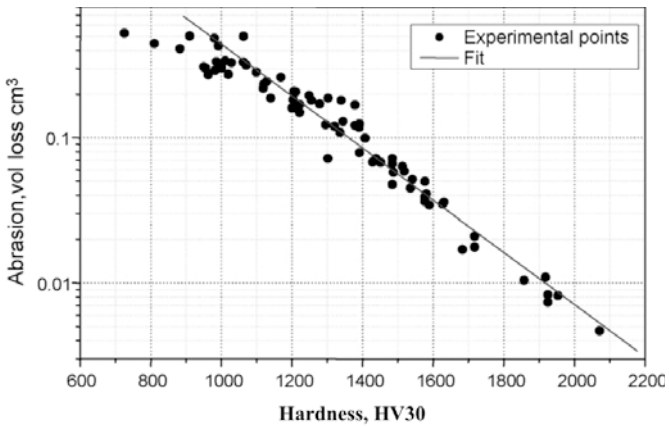

Fig. 2 : Variation of wear volume with hardness for ASTM B611 tests on range of hardmetals. The linear fit is for an expression of the type V = A exp(-BH) (reproduced from Ref.1).

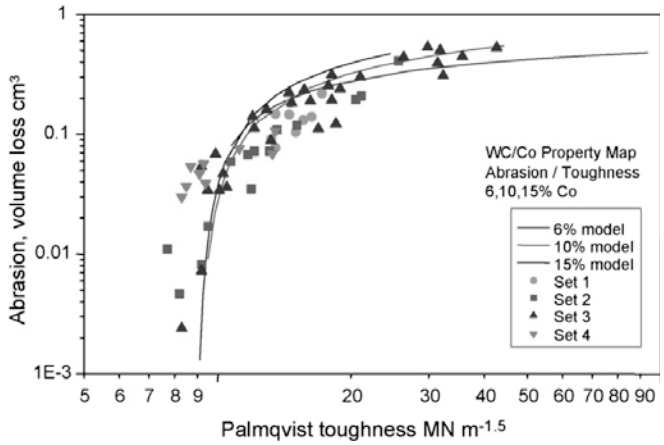

Fig. 3 : Dependence of abrasive wear volume (ASTM B611 tests) on Palmqvist toughness. Note that the different coloured points are different sets of WC/Co hard metals (reproduced from Ref.1).

be increased with a penalty in hardness by increasing the Co content. In contrast, a reduction in WC cuboid size with a concomitant decrease in inter-cuboid spacing normally increases both the hardness and toughness of WC-Co.

WC-Co cemented carbides have excellent resistance to abrasion and erosion which represent the most severe forms of wear encountered by engineering components in services. For example, Fig. 2 presents the data of Gee et al [1] on the abrasion rate of a wide range of WC based hard metals having hardness (HV30) in the range of 800 to 2100. It is very clear that the abrasion rate continuously decreases with increasing hardness of WC-Co. The same authors have also examined the influence of Palmqvist toughness of WC-Co on its abrasion rate (Fig. 3). Surprisingly, it can be observed Fig. 2, that toughness, unlike hardness, does not play an important role in determining the abrasion resistance.

The erosion resistance of WC-Co hard metal has also been investigated by numerous investigators. For example, the erosion data obtained by Ninham and Levy [2] over a wide range of carbide volume in a WC based system is illustrated in Fig. 4. Once again, there is a clear trend of decreasing erosion rate with increasing hardness. However,

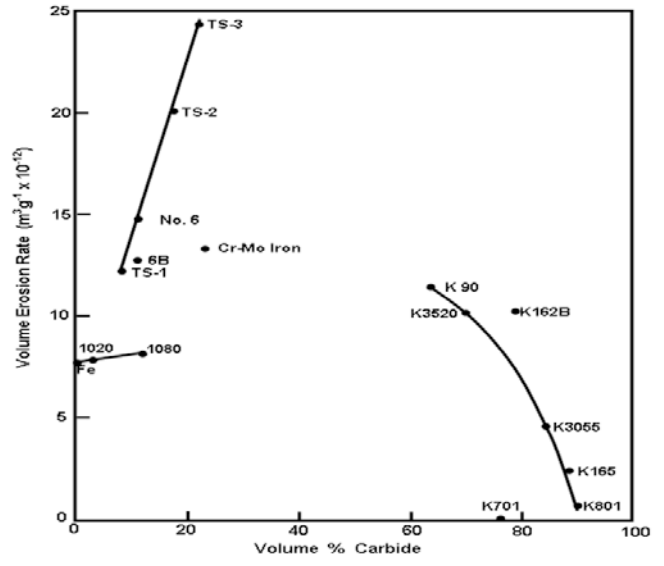

Fig. 4 : Plot of steady state erosion rate Vs. volume percentage carbide in the target (reproduced from Ref.2).

other investigators have noted that WC based Cermets should have adequate indentation toughness to perform well under erosion conditions [3-5].

On the basis of the above discussion, it can be concluded that in the case of bulk WC based Cermets, obtained by the liquid phase sintering route, hardness is the most important parameter which determines its resistance to abrasion and erosion. Indentation toughness is the next important parameter in that an adequate (minimum) level of toughness has to be ensured in the WC cermet, especially if it has to exhibit excellent resistance erosion.

However, it is important to note that in many applications requiring wear resistance, there is no requirement to make the whole component out of the costly WC based cermet. Rather, a thick WC based coating deposited on the component made from much cheaper material like steel should be an attractive option. In fact, thermal sprayed WC-Co coatings (up to a few hundred micrometer thick) have already established themselves for a large number of such applications. Among the available thermal spray techniques for obtaining wear resistant WC-Co coatings, High Velocity Oxy Fuel (HVOF) and Detonation Spray (DS) coating techniques are the most popular especially since they can result in thick and dense WC-Co coatings.

The main purpose of this article is to evaluate the WC-Co coatings obtained using detonation spray coating in comparison to bulk WC-Co of identical composition in terms of mechanical properties (hardness, modulus, toughness etc.) and more importantly discuss the additional property / process parameter requirements that have to be necessarily considered when a bulk WC-Co is replaced by a detonation sprayed WC-Co coating on a substrate / component.

2. Detonation spray coating process vis-à-vis liquid phase sintering

As indicated earlier, the bulk WC-Co cermet is usually obtained by liquid phase sintering. The time and temperature at which liquid phase sintering is carried out and the reducing atmosphere under which sintering is done ensures that only the Co binder undergoes melting and more importantly, the interaction between the molten Co phase and the solid WC cuboids is minimal. Thus, the final sintered WC-Co material (see Fig. 1) essentially consists of WC and Co phases as revealed by X-ray Diffraction studies [6]. The hardness (H) and the elastic modulus (E) of the sintered bulk WC-Co depends on the Co content and also on WC cuboid size. For example, as illustrated in Fig. 5a, the Vickers hardness of sintered WC-Co lies in the range HV 800 to HV 2300 while the elastic modulus spans the range 450 to 650 GPa [7-23]. The indentation fracture toughness of sintered WC-Co on the other hand decreases with increasing hardness of WC-Co (primarily due to a decrease in Co content) as illustrated in Fig. 5b. The toughness values of sintered WC-Co span the range 10 to 18 MPa $\sqrt{m}$ [5,7-14,16,20,22-24].

In contrast to liquid phase sintering, the coating formation is less controlled in the case of thermal spray coatings. In all the thermal spray techniques, the feed stock is in the form of powders (e.g. WC-Co powder) and they are entrained in the high velocity, high temperature gas/air stream. As the particles travel with the gas/air stream, they get heated up and also undergo acceleration. The nature of the thermal spray process and the powder particle size and density determines the final temperature and velocity of the powder particles prior to impacting the component surface. At one

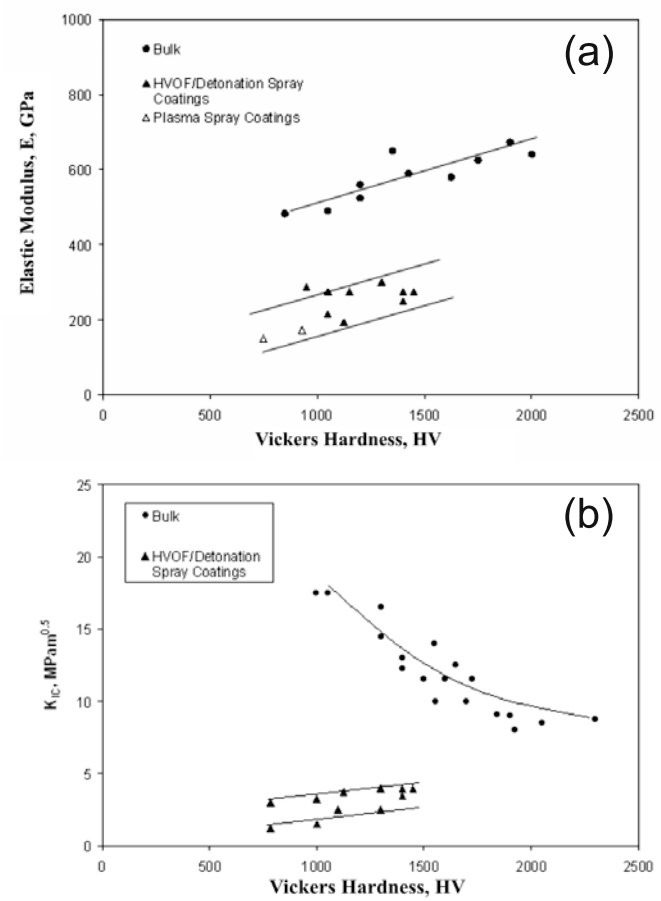

Fig. 5 : (a) Elastic modulus of bulk and thermal sprayed WC-Co coatings as a function of their respective Vicker's hardness. (b) Fracture toughness (K_{IC}) of bulk and thermal sprayed WC-Co coating as a function of their respective Vicker's hardness.

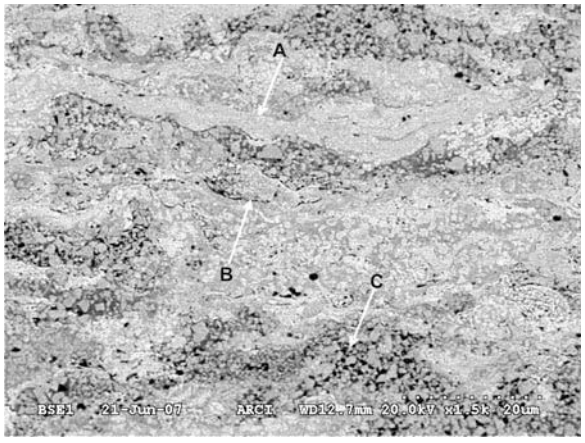

Fig. 6 : Cross-sectional SEM image (BSE mode) of detonation sprayed WC-Co coatings.

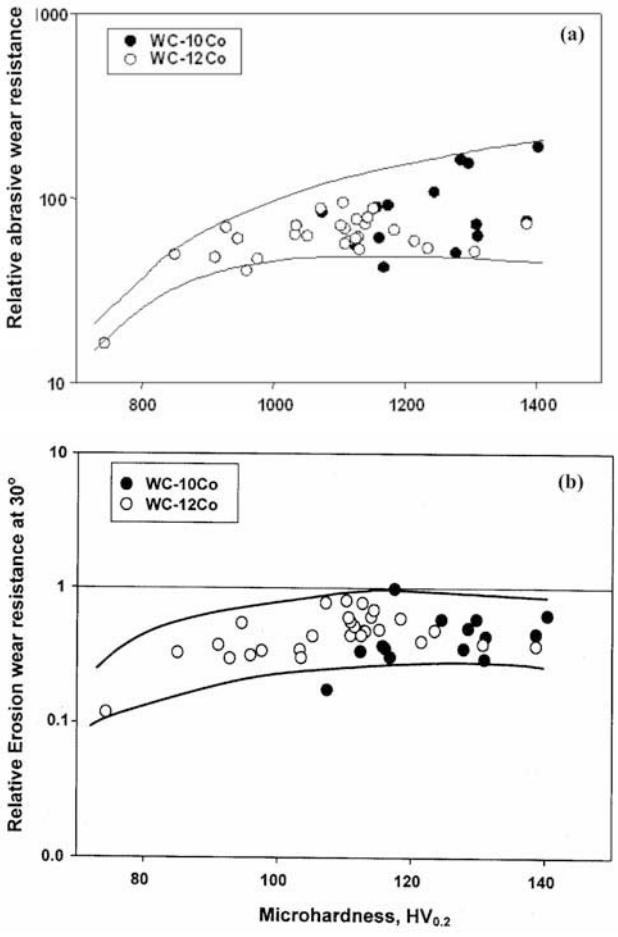

Fig.7 : (a) Relative abrasive wear resistance of detonation sprayed WC-Co coatings as a function of Vicker's hardness. (b) Relative erosive wear resistance of detonation sprayed WC-Co coatings as a function of Vicker's hardness.

extreme, air plasma spray results in extremely high particle temperatures such that WC-Co particles become molten during flight, but the WC-Co particle velocities are low in the range 100 to 150 m/s [25-28]. In contrast, in the case of detonation spray and HVOF coating techniques, the temperature of WC-Co particles lie in the range 1873 to 2573 K (i.e., the Co binder phase alone becomes molten during flight) while the WC-Co particle velocities lie in the range 500 to 800 m/s [25-28].

The semi-molten WC-Co particles then impact the component/substrate surface get deformed extensively to form disc shaped pancakes, which are usually called as "splats". Continuous impact of such particles result in the formation of thick layered coatings composed of splats superimposed over each other. A typical cross-sectional view of the detonation sprayed WC-Co coating is shown in Fig.6. The presence of splats with each splat representing one original powder particle is clearly evident. It is also clear that the intersplat boundaries are well-bonded in certain locations (see locations marked 'A' in Fig.6) but not bonded at all in certain other areas (see locations marked 'B' in Fig.6). In addition, presence of pores can also be observed at various locations (see areas marked 'C' in Fig. 6). Thus, it can be concluded that the detonation sprayed WC-Co coatings have a layered structure with a mix of both weak and strong inter-splat boundaries. Such a structure has enormous influence on the mechanical properties of the WC-Co coating since the weak inter-splat boundaries can be treated as cracks and the presence of numerous such cracks, parallel to the coating plane, can substantially reduce the elastic modulus and indentation toughness of WC-Co coatings [29-31]. In fact, in Figs. 5a and 5b, the modulus, hardness and toughness of WC-Co coatings are presented as filled triangles. Compared to bulk WC-Co (represented as filled circles in Figs. 5a and 5b), the elastic modulus of WC-Co coating is nearly half in value while toughness is lower by a factor of 4 or so.

The unusual layered structure of the detonation sprayed WC-Co coating is also reflected in its variable abrasion and

erosion properties, as illustrated in Figs. 7a and 7b. In these figures, the relative wear resistance (abrasion or erosion) is defined as the wear rate of the mild steel sample to the wear rate of the WC-Co coatings tested under identical test conditions and thus higher the value of relative wear resistance, better is the wear resistance of the WC-Co coating as compared to the mild steel substrate. It can be noticed from Figs. 7a and b, that in the case of detonation sprayed WC-Co coatings, the abrasion and erosion resistance is not strongly influenced by coating hardness. In addition, in the case of erosion of WC-Co, the absolute values of erosion rates of WC-Co coatings are comparable to that of the mild steel substrate (since the relative erosion resistance in Fig. 7b is of the order of 1). Such a poor performance of WC-Co coatings is obviously related to its layered structure composed of weak intersplat boundaries.

In conclusion, it can be stated that the bulk WC-Co and detonation sprayed WC-Co coatings are quite different from each other in terms of microstructure, mechanical properties and tribological behaviour.

3. Phase retention during detonation spray coating

As indicated earlier, liquid phase sintering of bulk WC-Co is carried out in a reducing atmosphere and also at a temperature which ensures dissolution of WC in molten Co is minimal. As a result, the phases present after sintering are essentially WC and Co. This in turn results in outstanding mechanical properties (see Fig.5) since the soft Co binder surrounds the hard WC cuboids creating the classical composite effect.

In contrast, in the case of detonation spraying, the high velocity, high temperature gas stream in which the powder particles are entrained is essentially the product of the combustion reaction (of fuel (acetylene) and oxygen) and thus can be oxidizing or slightly reducing depending on the ratio of fuel to oxygen. In addition, the near surface region of the WC-Co powder particle can reach temperatures as high as 2573 K. As a result, Co binder phase surrounding the WC cuboid in the near surface regions of the particle, undergoes not only melting but also gets superheated enhancing the dissolution of WC into the Co phase.

The sequence of events following the dissolution of WC into the Co phase has been investigated by the present authors [32] by carrying out detonation sprayed coating of WC-Co coating over a range of oxygen-fuel (OF) ratios. These investigations reveal that the WC cuboids become rounded and smaller due to dissolution in the Co matrix. As a consequence, given the extensive solubility of both W and C in Co at elevated temperatures, Co matrix becomes rich in W and Co. However, the extent of retention of the dissolved C in Co is determined by the rate at which C is lost from the Co matrix due to the formation of CO_2/CO by reaction with O_2 in the gas stream surrounding the powder particle. In the next phase, as the powder particles cool rapidly upon impacting the substrate (resulting in coating formation), the solubility of both W and C decreases dramatically. This in turn results in the precipitation of W_2C on WC cuboids (W_2C shell around WC cuboids) and W in dendritic form. The relative proportion of W_2C and W formed thus depends on the extent to which C has been retained in Co matrix which in turn depends on the oxygen to fuel (OF) ratio used while carrying out the detonation coating process.

Consistent with the sequence of events described above are the backscattered SEM images of the WC-12Co coatings deposited at oxyfuel ratio of 1.16 (Fig. 8a), 1.50 (Fig. 8b) and 2.0 (Fig. 8c & d). At an OF ratio of 1.16, resulting in the least oxidizing atmosphere around the powder particles, the WC cuboids retain their sharp edges and the Co matrix is nearly pure and does not contain W or C in solution (Fig. 8a). In

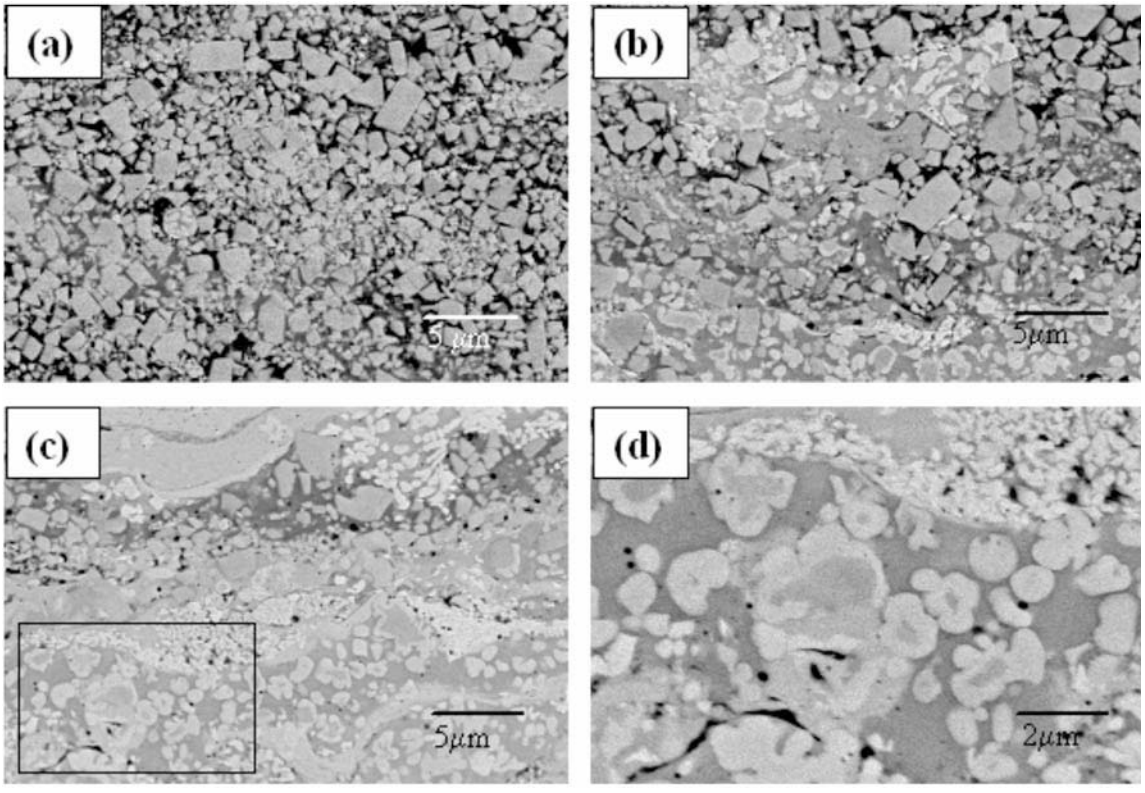

Fig. 8 : Backscattered SEM images of WC-12Co coatings deposited by detonation spray technique at various oxy fuel ratios (a) 1.16; (b) 1.5; (c) 2.0 and (d) higher magnification of inset in (c) showing the rim like structure around the WC cuboids embedded in the W rich Co matrix.

contrast, at OF ratios of 1.5 and 2.0 (more oxidizing atmospheres), the coatings are composed of bands of alternative regions with bright and dark background as can be observed from Fig. 8b and 8c. The band with the dark background is identical to Fig. 8a (OF: 1.16) and represents the region which has not undergone decarburisation. On the other hand, the regions with the bright background in Figs. 8b and 8c represent the decarburised region of the coating and are characterized by rounded WC grains and also the Co phase rich in W and C (that is why the Co phase also looks bright). A comparison of Figs. 8b and 8c also clearly indicates that the extent of bright regions is substantially more in the coatings obtained at OF ratio 2.0 (very oxidizing) as compared to the coatings obtained at OF ratio of 1.5 (moderately oxidizing). A higher magnification view of the coatings obtained at OF ratio of 2.0 (Fig. 8d) clearly indicates the presence of W_2C shell on the original WC cuboid. Thus, it can be concluded that as the ratio of oxygen to fuel in the input gas fed to the detonation coating system increases from 1.16 to 2.00, more extensive is the decarburisation of the WC-Co coating causing an increase in the content of W_2C and W phases at the expense of the desired WC phase and also more is the formation of less ductile Co binder phase due to incorporation of W and C. The actual contents of the various phases in the WC-Co coating and also its extensive decarburisation with increasing OF ratio is clearly brought out in Table 1.

Apart from oxy-fuel ratio, another parameter which can influence phase integrity is the particle size of the starting powder. As the powder particle becomes finer, the surface area available for interaction with the surrounding oxidizing gas increases substantially, thereby leading to an effect similar to increasing the oxygen to fuel ratio in the feed gas. This particular aspect has been investigated for a variety of powders by Suresh Babu et al [23]. Their results pertinent to WC-12Co powder are presented here. Figure 9 shows the SEM images of the three fractions of WC-12Co powders used while Fig. 10 illustrates their cumulative particle size distribution. The relative proportions of the WC and W_2C phases present in the coatings (as measured using XRD) obtained using the three fractions mentioned above and at an OF ratio of 1.16 (least oxidizing) is presented in Fig. 11. It is clear that as the mean powder size decreases, more is the decarburisation, as indicated by increasing content of the W_2C phase at the expense of the WC phase.

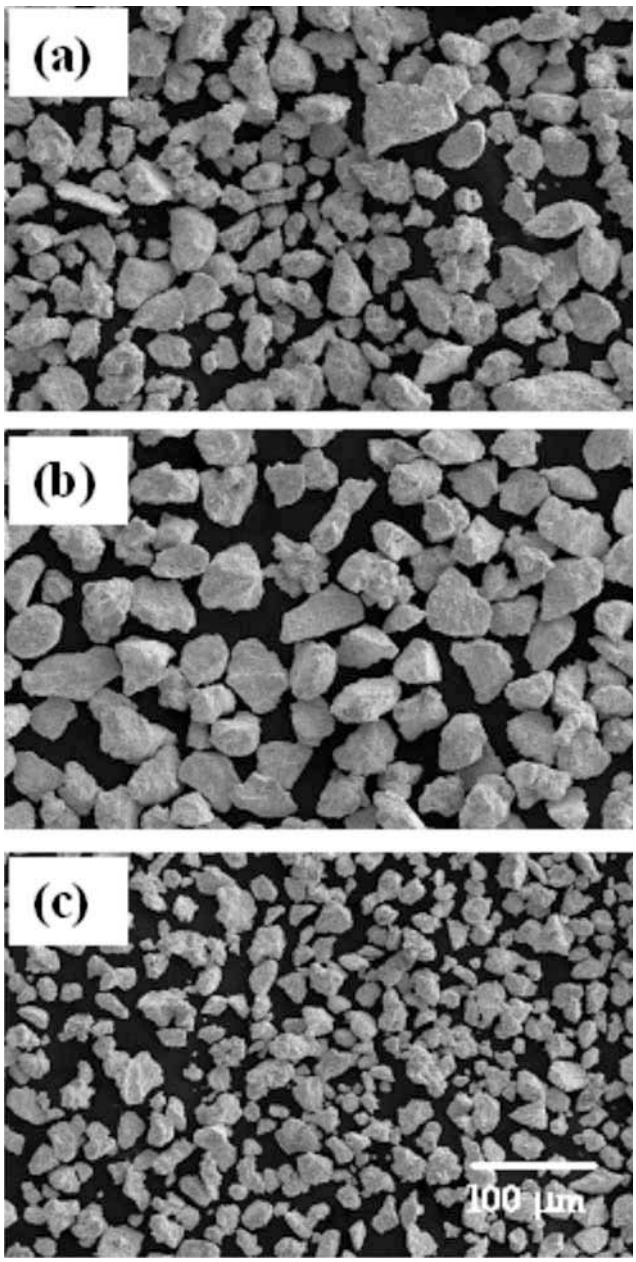

Fig. 9 : SEM images of WC-12Co powder. (a) as-received powder; (b) coarse powder; (c) fine fractions of the powder.

Table 1 : Influence of OF ratio on the decarburisation of WC-12Co Coatings

Phases	*Percent phases present*			
	Feed stock (starting powder)	*Coating*		
		OF : 1.16	*OF : 1.50*	*OF : 2.0*
WC*	100	97	58	45
W_2C*	-	3	22.5	23.5
W*	-	-	19.5	31.5
Co (pure) **	100	87	34	20
Co (with C&W) **	-	13	66	80
% decarburisation+	0.0	4.4	34.0	45.0

* From XRD, assuming that the percent of WC, W_2C and W adds up to 100%.

** From SEM based image analysis assuming Co phase which appears gray is pure while Co phase which appears bright is rich in W and C. It is assumed that pure Co phase and W rich Co phase adds up to 100%.

\+ Estimated by using Leco carbon analysis. % decarburisation defined with respect to the starting powder.

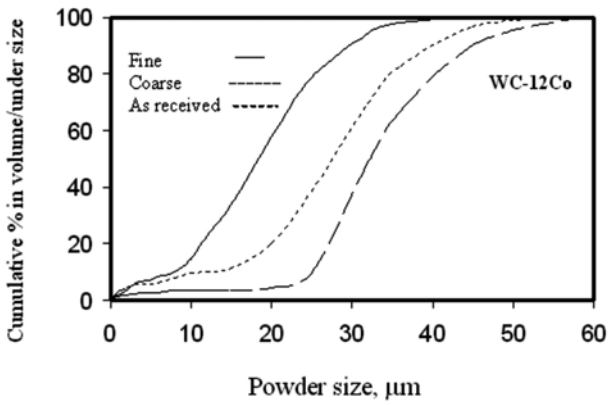

Fig. 10 : Cumulative size distribution curves of WC-12Co powder.

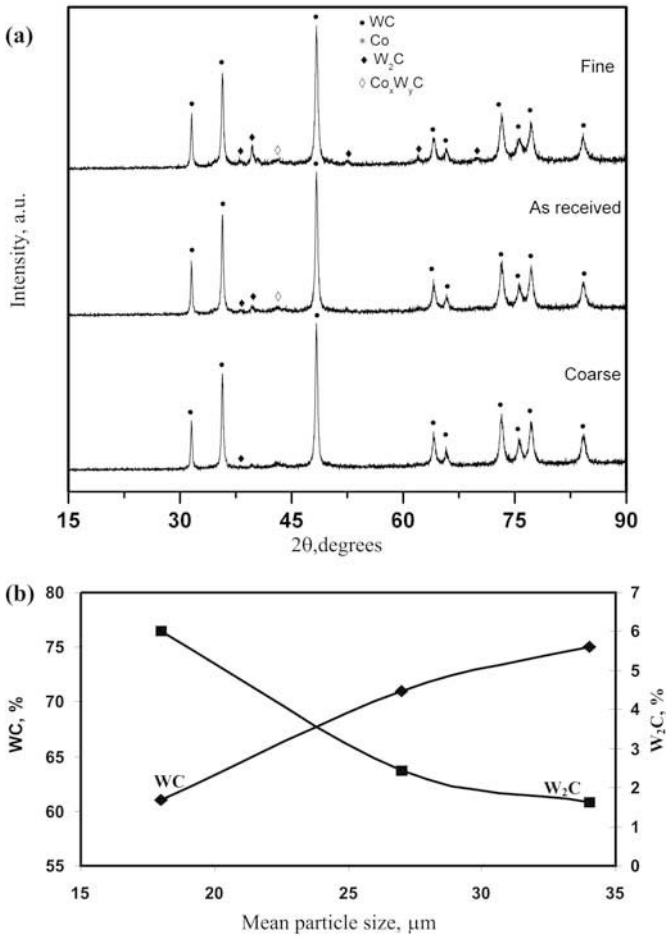

Fig. 11 : X-ray diffractions patterns (a) and phases present as a function of feedstock size (b) of WC-12Co coatings.

In conclusion, it can be stated that while the sintering atmosphere and temperature and time of sintering are very well chosen and controlled during liquid-phase sintering of WC-Co thereby avoiding dissolution/decarburisation of the WC phase, such is not the case with detonation spray coating process. In the coating process, neither the temperature and atmosphere of the gas surrounding the particle nor the time of interaction between the particle and the surrounding gas (which depends on particle velocity which in turn is determined by the particle size and density) are controlled. As a result, the retention of the original, desired phases present in the powder particle in the coating which is formed is both difficult and not controllable. This, in turn, invariably results in a deterioration in properties and performance of the WC-Co coatings as compared to bulk WC-Co as indicated earlier (Fig.5).

4. Additional interface-related property requirement for WC-Co coatings

In the last section, we have discussed the reasons for the inferior performance of WC-Co coatings compared to its bulk counterpart. However, the introduction of a thick coating on a substrate, introduces additional features related to the nature of bonding between the coating and the substrate. In the case of detonation spray coating (as in all thermal spray coatings), the adhesion between the coating and the substrate is due to mechanical "interlocking" caused by the roughness of the substrate. Therefore, prior to detonation spray coating, the substrate has to be roughened considerably by shot blasting.

In view of the above, if the WC-Co coating-substrate adhesion is weak, coating will perform poorly even though coating per se may have the optimum microstructure and excellent properties. On the other hand, if the inter-splat bonding is poor, coating will again perform poorly though it might have an optimum intra-splat properties. Thus, it is important to evaluate the properties of the coating-substrate to ensure that they are adequate to prevent the failure of the coating at the coating-substrate interface. In this section, recently developed experimental techniques to assess the strength of the bond between the coating and substrate and the toughness of the interface between the coating and substrate will be presented.

4.1 Evaluation of coating-substrate bond strength

Several methods have been developed over the years to measure the coating-substrate bond strength. The most common/popular test technique used by the thermal spray community for evaluation of the bond strength is the direct tensile pull-off test as per ASTM standard C633-79. A schematic view of the experimental set up is illustrated in Fig. 12. First, the coating of the required thickness is applied on the face of a cylindrical test specimen of diameter 25.4 mm and 25.4 mm long. The coated face of the cylindrical specimen is bonded to another cylindrical specimen of identical dimensions but without any coating applied. The bonding is achieved using an epoxy tape placed between the faces of the 2 cylindrical specimens (one coated and the other bare) and then curing the epoxy tape (with the samples) by heat treatment. The specimen-epoxy tape set up is next pulled in tension till the two cylindrical specimens separate. The load at which the separation occurs divided by the face area gives the bond strength provided the failure occurs at the coating-substrate interface. On the other hand, if the samples separate along the epoxy-substrate interface, the reported bond strength is that of the epoxy-sample interface and hence not useful. Given the fact that the best available epoxy tapes can measure bond strengths up to a maximum value of 70 MPa, the above test is adequate to measure the bond strength of flame sprayed and air plasma sprayed coatings (their bond strengths are usually lower than 70 MPa), but not detonation sprayed coatings wherein the bond strength exceeds 70 MPa.

In view of the above, a new pin type test established by ARCI collaborator (Institute for Problems in Material Sciences, Kiev), which avoids the use of epoxy tape has been

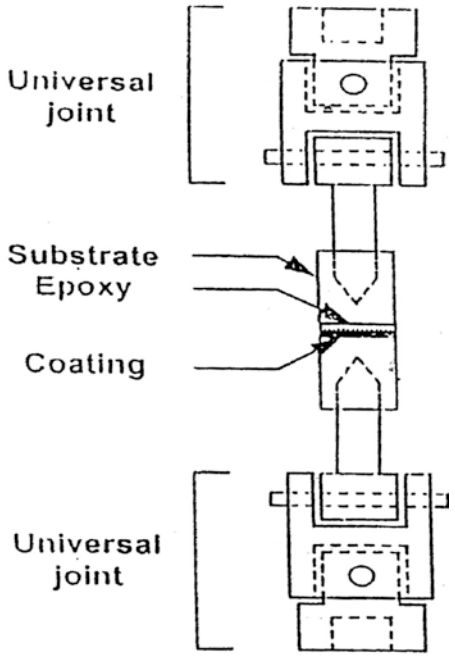

Fig. 12 : Direct tensile Pull-Off adherence test as per ASTM C633-79.

developed. The specimen and test details are provided in Fig. 13 a & b. In this method, a tapered hole is first machined through the substrate sample from its backside prior to applying the coating. A tapered plug of the substrate material is then fabricated such that when this plug is inserted into the tapered hole made on the substrate sample (from backside) it fits perfectly in the hole and the front face of the tapered plug is flush with the face of the substrate sample as shown in Fig. 13a. The substrate sample with the plug is then housed in a special device as shown in Fig. 13a. This

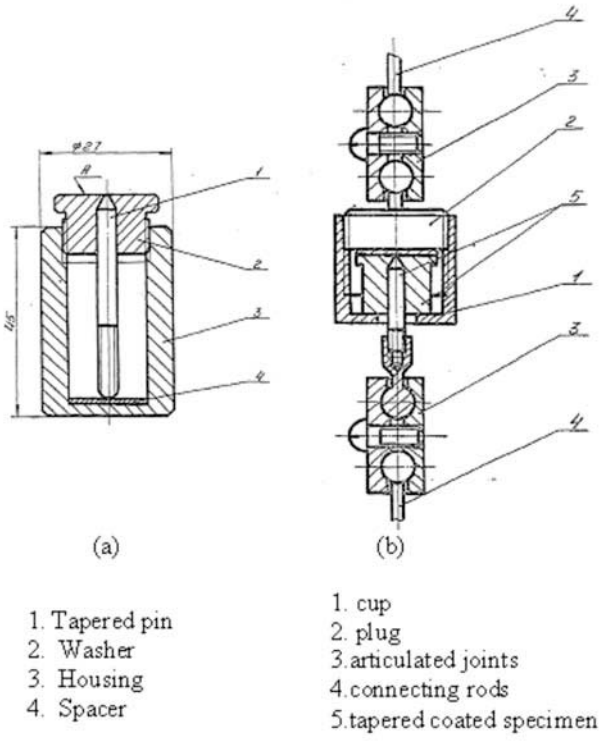

Fig. 13 : (a) A tapered washer along with pin housed in a special device. (b) Laboratory set-up for determining bond strength of thermal sprayed (reproduced from IPMS, Kiev).

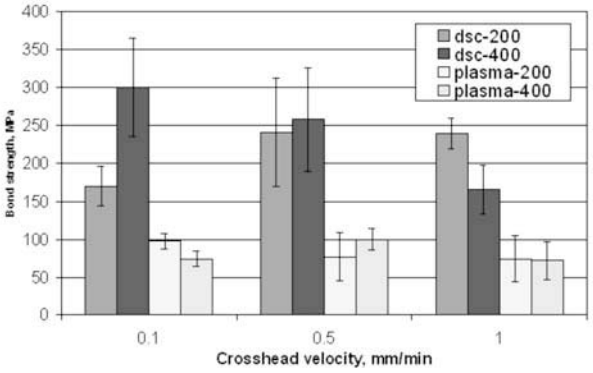

Fig. 14 : Effect of coating thickness, crosshead velocity and spray technique on the bond strength of WC-Co coatings.

assembly is then subjected to cleaning, grit blasting and coating deposition. Next, the assembly is fixed in the tensile testing machine as illustrated in Fig. 13b and the tapered plug is then pulled away from the coating. The load/force at which the tapered plug breaks free from the coating divided by the tapered plug face area gives the tensile bond strength of the coating-substrate interface.

The authors have recently carried out bond strength studies, as per the above technique, on a wide variety of detonation sprayed coatings and also on coatings obtained using different thermal spray technique. The results pertinent to WC-Co coatings obtained by both detonation spray and air plasma spray techniques are presented in Fig. 14. The first point to be noted is that detonation spray coatings are characterized by substantially higher bond strength as compared to air plasma spray. The bond strength of detonation sprayed WC-Co coatings lie in the range from 150 to 300 MPa which is much higher than the strength of 70 MPa of the best epoxy tape available. In contrast, air plasma sprayed WC-Co coatings exhibit bond strengths in the range 50 to 100 MPa. In the case of detonation sprayed WC-Co coatings, the coating thickness (200 Vs. 400 μm thick) has an effect on bond strength while in plasma sprayed WC-Co, the effect of coating thickness on bond strength is marginal. The cross-head velocity at which the bond strength test is carried out (in a tensile testing machine) also has an influence on the measured bond strength values, though it is hard to rationalize these results at this stage.

4.2 Coating-substrate interface toughness

A new indentation test procedure suggested by Chicot et al [33,34], allows the estimation of fracture toughness of the coating-substrate interface. In this technique, the coated sample is sectioned and polished and then a Vickers indentation is placed exactly on the interface between the coating and the substrate as illustrated in Fig. 15. Under such indentation conditions, the cracks invariably propagate from the corners located at the interface (i.e. corners *m* and *o*) but not from corners located away from the interface (i.e., corners *n* and *p*) since interface is always weaker and thus provides ready path for crack initiation and propagation. This aspect is clearly illustrated in Fig. 16.

Detonation sprayed WC-Co coatings result in a very tough interface (with the substrate) and therefore, the technique described in this section is unsuitable for measuring interface toughness of such a material. As a result, the data presented in this section pertains to detonation sprayed Cr_3C_2-25NiCr coatings. The test procedure

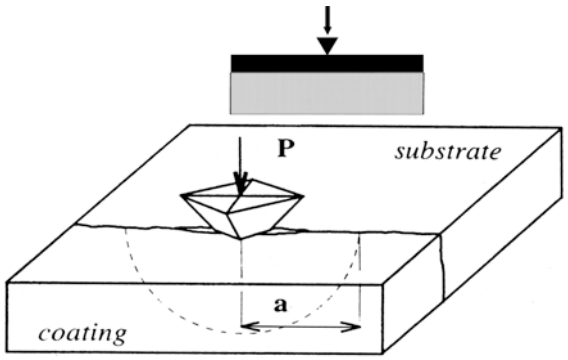

Fig. 15 : Schematic diagram showing the indentation at the interface (reproduced from Ref. 33, 34).

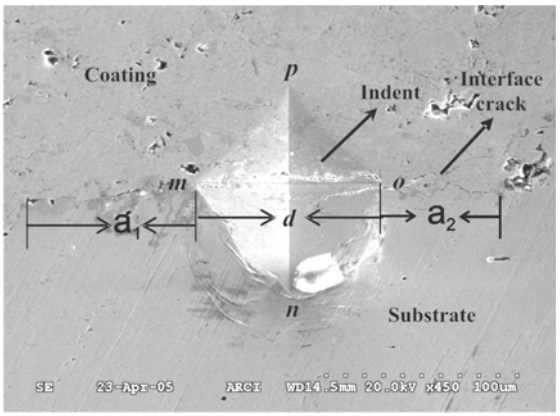

Fig. 16 : Typical SEM image of Cr_3C_2-25%NiCr coating with indent at interface and the interface cracks propagating from the corners (*m* and *o*) located at the interface.

is as follows. Indentations are carried out at the interface over a range of loads and the average crack length ($a = (a_1 + a_2)/2$; see Fig.16) is measured for each load (P). The relationship between a and P is then obtained as indicated in Fig. 17a. In this figure, the filled diamond (◆) symbols represent the indentation diagonal (d in Fig. 16) Vs. load (P) data and the best-fit line of this data is designated as "apparent hardness". The other 3 lines in Fig. 17a represent the a Vs. P data for detonation sprayed Cr_3C_2-25NiCr coatings of three different thicknesses (filled circles (●) : 220 μm thick; upward triangle (▲) : 305 μm thick and filled squares (■): 415 μm thick). The extrapolation of a – P data points backwards results in its intersection of the apparent hardness line. The P and a value corresponding to this intersection point is designated as P_c and a_c (i.e. critical value of P and a at crack initiation) and using these values, interfacial fracture toughness (K_{ca}) is obtained as [33,34],

$$K_{ca} = 0.015 \frac{P_c}{a_c^{3/2}} \left(\frac{E}{H}\right)_i^{1/2} \quad (1)$$

In equation 1, the ratio of modulus to hardness at the interface [i.e. $(E/H)_i$] is obtained using the relation [33,34],

$$(E/H)_i^{1/2} = \left[\frac{(E/H)_S^{1/2}}{1+(H_S/H_C)^{1/2}}\right] + \left[\frac{(E/H)_C^{1/2}}{1+(H_C/H_S)^{1/2}}\right] \quad (2)$$

In equation 2, the subscripts *i, S* and *C* stand for interface, substrate and coating respectively.

The K_{Ca} values obtained in the above manner for detonation sprayed Cr_3C_2-NiCr coating on a mild steel substrate, for three different coating thickness values, is presented in Fig.17b. It is clear from this figure, wherein K_{Ca} is plotted against $1/t^2$ (where t = coating thickness), that the coating-substrate interface toughness of detonation sprayed Cr_3C_2-NiCr coating increases with increasing thickness. In fact, if we extrapolate the K_{Ca} data in Fig.17b to "infinite" t value (i.e. $1/t^2 = 0$), the resulting K_{Ca} value designated as K_{CaO}, represents the intrinsic interface toughness when the coating is infinitely thick. For the detonation sprayed Cr_3C_2-NiCr coating, K_{CaO} value is 5.37 MPa√m while the values of K_{Ca} for coatings of thickness 220, 305 and 415 mm equal 1.42,3.04 and 4.44 MPa√m respectively.

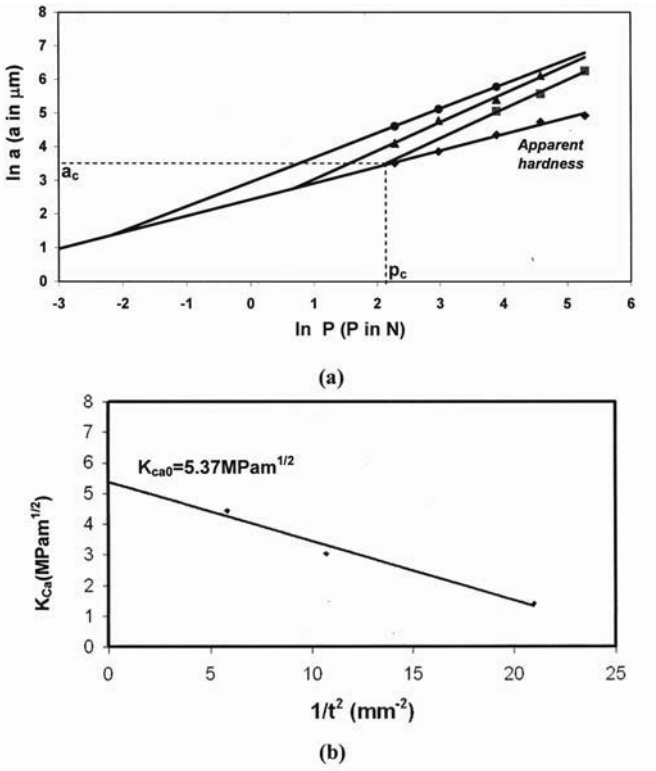

Fig. 17 : (a) Bi-logarithmic representation of relationship between the crack length (a) and indentation load (P) for Cr_3C_2-25%NiCr coatings. (b) Influence of coating thickness (t) on the apparent interfacial toughness (K_{Ca}) and estimation of intrinsic interfacial toughness (K_{Cao}).

5. Conclusions

In this paper, the unique aspects related to the structure and mechanical behaviour of detonation sprayed WC-Co coatings has been highlighted and contrasted with that of liquid phase sintered WC-Co cermet. It has been shown that the hardness and toughness of WC-Co coatings are substantially lower than that of bulk WC-Co cermet primarily due to the layered nature of the coating structure characterized by porosity and weak inter-splat boundaries. It has also been demonstrated that the phases present in the coating depends critically on the process parameter used (e.g. oxygen to fuel ratio) while carrying out the detonation spray coating but also on the size of the powder particle used as feed stock. In addition, it has also been pointed out that the introduction of an interface between the WC-Co coating and the substrate brings forth additional concerns related to the bond strength and toughness of the coating-substrate interface and the methodology for evaluating these interface-related properties has been described in detail.

Acknowledgements

The authors are grateful to the staff of Centre for Engineered Coatings (ARCI) and Centre for Mechanical and Microstructural Characterization (ARCI) for their assistance in coating deposition and characterization. One of the authors would like to thank Mr. S. Abdul Azeez Raja and Ms. A Parvathi for their kind assistance in bond strength and interface toughness experiments.

References

1. Gee M G, Gant A and Roebuck B, *Wear,* **263** (2007) 137.
2. Ninham A J and Levy A V, *Wear,* **121** (1988) 347.
3. Hutchings I M, *Tribology: Friction and Wear of Engineering Materials,* Edward Arnold, London, (1992) p 171.
4. Cantera E L and Mellor B G, *Mater Lett* **37** (1998) 201.
5. Lima M M, Godoy C, Modenesi P J, Avelar-Batista J C, Davison A and Matthews A, *Sur. Coat. Technol.,* **177-178** (2004) 489.
6. Park S J, Cowan K, Johnson J L and German R M, *Int J Refra Met. Hard Mater.,* **26** (2008) 152.
7. Allen C, Sheen M, Williams J and Pugsley V A, *Wear,* **250** (2001) 604.
8. ASM Hand book Vol. 2. Properties and selection of non-ferrous alloys and special purpose materials.
9. Fang Z, Lockwood G and Griffo A, *Metall. Mater. Trans. A,* **30** (1999) 231.
10. Ponton C B and Rawlings R D, *Mat. Sci. Techno.,* **5** (1989) 961.
11. ASM Engineered Materials Reference Book, *ASM International*, (1989).
12. Saito H, Iwabuchi A and Shimizu T, *Wear,* **261** (2006) 126.
13. Fang. Z Z, *Int J Refra Met. Hard Mater.,* **23** (2005) 119.
14. Jia K, Fischer T E and Gallois B, *NanoStruct. Mat.,* **10** (1998) 875.
15. Pirso J, Letunovits S and Viljus M, *Wear,* **257** (2004) 257.
16. Schubert W D, Neumeister H, Kinger G\ and Lux B, *Int J Refra Met. Hard Mater.,* **16** (1998) 133.
17. Hussainova I, *Tribo Int*., **34** (2001) 89.
18. Factor M and Roman I, *J. Therm. Spray Technol* **11** (2002) 468.
19. Cashon E P, *Tribo Int* **8** (1975) 111.
20. Chivavibul P, Watanabe M, Kuroda S and Shinoda K, *Surf Coat Technol* **202** (2007) 509.
21. Tucker R C Jr, *J Vac Sci Technol* **11** (1974) 725.
22. Yang Q, Senda T and Ohmori A, *Wear* **254** (2003) 23.
23. Suresh Babu P, Rao D S, Rao G V N and Sundararajan G, *J Therm Spay Technol* **16** (2007) 281.
24. Lima M M, Godoy C, Avelar-Batista J C and Modenesi P J, *Mat Sci Eng* **357 A** (2003) 337.
25. Morks M F, Gao Y, Fahim N F and Yingqing F U, *Mater Lett* **60** (2006) 1049.
26. Kharlamov Y A, *Thin Solid Filml* **54** (1978) 271.
27. Marple B R , Voyer J, Bisson J F and Moreau C, *J Mater Pro Technol* **117** (2001) 418.
28. Srinivasa Rao D, Sen D, Somaraju K R C, Ravi Kumar S, Ravi N and Sundararajan G, *Proc of 15th ITSC, France* (1998) 385.
29. Li C J, Ohmori A and Mc Pherson R, *J Mat Sci* **32** (1997) 997.
30. Leigh S H and Berndt C C, *Acta Mater* **47** (1999) 1575.
31. Nakamura T, Qian G and Berndt C C, *J Am Ceram Soc* **83** (2000) 578.
32. Suresh Babu P, Basu B and Sundararajan G, *Acta Mater* **56** (2008) 5012 .
33. Lesage J and Chicot D, *Sur Eng* **15** (1999) 447.
34. Chicot D, Demarecaux Ph and Lesage J, *Thin Solid Film* **283** (1996) 151.